A REVIEW OF AERONAUTICAL FATIGUE INVESTIGATIONS IN ISRAEL

APRIL 1999 – MARCH 2001

Compiled by:
Abraham Brot
Engineering Division
Israel Aircraft Industries
Ben-Gurion Airport, Israel

SUMMARY

This review summarizes fatigue and fracture-mechanics investigations that were performed in Israel during the period April 1999 to March 2001. The review includes contributions from Israel Aircraft Industries Ltd. (IAI), Israel Air Force (IAF), Technion – Israel Institute of Technology, Tel-Aviv University and Ben-Gurion University.

Presented at the 27th ICAF Conference
Toulouse, France
26 June 2001

TABLE OF CONTENTS

A REVIEW OF AERONAUTICAL FATIGUE INVESTIGATIONS IN ISRAEL APRIL 1999 – MARCH 2001

11.1 INTRODUCTION

The Israel National Review summarizes work performed in the field of aeronautical fatigue in Israel during the period April 1999 to March 2001. The previous National Review [1] covered aeronautical fatigue activities up to March 1999. The following organizations contributed to this review:

Israel Aircraft Industries Ltd. (IAI)
Israel Air Force (IAF)
Technion – Israel Institute of Technology
Tel-Aviv University
Ben-Gurion University

The National Review was compiled by Abraham Brot of IAI.

11.2 FATIGUE ANALYSIS AND LIFE EXTENSION

11.2.1 Bounds on the Fatigue Threshold in Metals (J. Tirosh and S. Peles, Technion)

A theoretical approach was used for bounding the threshold stress amplitudes of fatigue crack growth, based on the shakedown theorems of Melan and Koiter. An elastic-perfectly-plastic material is considered which undergoes a fluctuating load, and may possess a residual stress field. Spherical inclusions are assumed which perturb the homogenous stress field and, at a certain threshold stress amplitude, trigger the propagation of cracks as a result of plastic deformation. This investigation succeeded in formulating the shakedown bounds for such a fatigue threshold amplitude. Experimental data for the fatigue threshold of various metals, flaw sizes and residual stresses were shown to fall reasonably well between the proposed upper and lower bounds. The results of this investigation were published [2].

11.2.2 Optimum Laser Treatment of Metals (E. Altus and E. Konstantino, Technion)

This investigation is a continuation of work reported upon in the Israel National Review that was presented to the 26th ICAF Conference [1]. In the present study, fatigue damaged Ti-6Al-4V alloy specimens were subjected to a Laser Surface Treatment (LST) using a 1.8 kW CW CO_2 Laser, and then were tested to failure. The intensity and LST time were varied in order to determine the optimum treatment. Two basic mechanisms for improving the fatigue life were identified: a Healing Mechanism (HM) which "erases" prior fatigue damage and a Microstructure Mechanism (MM) which modifies the material microstructure and, thereby, enhances its fatigue life. HM was found to be effective for surface temperatures above 400°C. MM was effective below 600°C and for specific laser conditions. The combination of both mechanisms led to an optimal LST of 2 seconds and 0.85 kW/cm^2. This optimal LST resulted in full healing as well as a mean fatigue life increase of 50% [3], [4]. The effect of LST exposure time on fatigue life is shown in Figure 1.

11.2.3 Development of a Two-Term Method for Predicting Fatigue Life (S. Peles and M. Weiss, Technion)

A series of investigations were performed by these authors [5] – [8], all dealing with the development of a fatigue life prediction model. The model is based on the assumption that various fatigue mechanisms, that have often been observed, are caused by different fatigue regimes. In certain cases, the different regimes exist concurrently in the same fatigue zone and each one causes the crack to propagate independently. Figure 2 shows the fatigue domain divided into fatigue and fracture regimes and into six zones. Each zone exhibits different fatigue and fracture characteristics. In cases where different fatigue regimes exist concurrently in the same fatigue zone, crack growth calculations include the superpositioning of the separate phenomena.

The model is composed of two crack growth expressions. The first expression is based on the stress-intensity range as the main parameter, which is appropriate for determining the crack growth rate of large cracks. The second expression is proportional to the cyclic plastic zone size, and determines the crack growth rate for both short and long cracks. The model was first introduced by M. Weiss in 1992, but has been extended significantly in recent years.

The two-term fatigue life prediction model has been shown to result in life predictions for AISI 4340 low alloy steel, 2024-T4 and 7075-T6 aluminum specimens, which compare well with experimental results. The effect of a mean stress environment has been incorporated into the model by means of the Gerber relation. The threshold stress-intensity factor range has been modified as a function of the stress ratio, R, using an approach based on the shakedown theorems of Melan and Koiter. It is shown that all the parameters of the two-term model can be calculated, based on basic fatigue material constants.

The model has recently been extended by incorporating the crack closure effect into the calculations [7]. A recent study has been completed thereby justifying the method based on first principles, using a semi-analytic derivation of the model [8]. These recent developments effectively transform the model from a theory into a justified set of equations.

11.2.4 Cracking of Autofrettaged Thick-Walled Cylinders (M. Perl et al, Ben-Gurion University)

A series of investigations were performed all dealing with thick-walled cylindrical pressure vessels [9] – [13]. These investigations are a direct continuation of work that was presented in the previous Israel National Review [1]. Although this work does not deal strictly with aeronautical fatigue, it was included in this review because the autofrettage technique is very similar to the cold-expansion method used extensively in the aircraft industry.

A method for measuring the level of autofrettage in a thick-walled cylinder was developed, using the classical split-ring experimental procedure as well as an axisymmetric stress release method that had been previously developed by the author [9]. The method combines the simplicity of the split-ring experimental method with the sensitivity and accuracy of the axisymmetric stress release approach. In addition, the built-in redundancy of measuring the released strain at two points as well as the opening angle, results in better control of the experimental procedure. The improved method includes a step-by-step algorithm for implementing the procedure.

The stress-intensity of a semi-elliptical crack emanating from an erosion at the bore of an autofrettaged pressurized cylinder was studied using a three-dimensional finite-element analysis using ANSYS 5.2 code [10]. The effect of autofrettage was simulated by an equivalent thermal stress field. Stress-intensity factors were determined by the modal displacement method. The solutions were studies parametrically for various erosion curvatures, crack depths and crack shapes. The results show that, under certain circumstances, the expected fatigue life can be reduced significantly due to the erosion of the bore. It is also concluded that a two-dimensional finite-element analysis could yield an unconservative estimate of the cylinder's fatigue life.

In another investigation, the effect of thermal shock on semi-elliptical cracks that may be present at the cylinder bore, was studied [11]. Typically, this could occur during the firing of a gun on a military aircraft. A transient stress-intensity factor resulting from the thermal shock loads was calculated using a three-dimensional finite-element analysis. Results were calculated for various crack arrays ranging from two cracks up to 48 cracks, for several typical geometries, and transient time steps. The results show that the stress-intensity is typically negative, thereby reducing crack growth rate.

In a related activity, the effect of machining an autofrettaged cylinder on the residual stress field was investigated [12]. The manufacturing process of gun barrels requires machining of both the bore and the outer surface to their final dimensions after the autofrettage process was performed. A closed-form analytical solution for the redistributed residual stress fields, resulting from the machining operation, was produced. For partially autofrettaged cylinders, it was found that machining of the bore reduces the overstrain level while machining of the outer surface increases the overstrain level.

In another activity, three-dimensional finite-element models were built to study stress intensity distributions for arrays of cracks along the bore of an autofrettaged cylinder [13]. The ANSYS 5.3 Finite-Element Code was used for the study. The number of cracks ranged from one to 180. More than 200 different combinations of crack depth, crack shape and levels of autofrettage were studied parametrically. The results clearly showed the importance of autofrettage in reducing the effective stress intensity factor. A follow-up investigation is underway, in which the combined effect of autofrettage and internal pressure will be studied.

11.2.5 Fatigue Life Analysis of a Cannon Barrel (L. B. Sills and R. Eliasi, Tel-Aviv University)

In order to determine the fatigue life of a steel cannon barrel, a finite-element analysis was performed to determine the stress intensity factor as a function of crack length. [14]. Two symmetrically located cracks were assumed. A statistical Monte Carlo analysis was performed, with many of the parameters assumed to be random variables, in order to determine the fatigue life of the cannon. The fatigue life of the barrel was modeled by the *Gumbel Extreme Value* distribution. The results of this investigation predicted that, for its required service life, the cannon will have a reliability of 99.999% with a confidence level of 90%.

11.3 FAILURE PREDICTION AND RELIABILITY

11.3.1 Assessing the Reliability of Fail-Safe Structures (A. Brot, IAI)

Fail-safe structures have been used for many years in aviation in order to enhance the reliability of aircraft structures. Even after the introduction of the damage-tolerance regulations in the 70s, which no longer required fail-safe design features, many primary aircraft structures continued to be designed for fail-safety. Recently, there have been proposals made to reinstate fail-safe requirements in the FAR-25 and JAR-25 Regulations.

Fail-safe structural concepts for aircraft appear to be very attractive. Failure of any single member will not result in the total failure of the aircraft. However, upon a closer examination, the weakness of the fail-safe concept emerges. Fail-safety can only be reliable if the operator is aware that a structural member has failed. Under the present state-of-the-art, this is accomplished by performing periodic inspections in order to detect the failure of a structural member. These inspections result in aircraft downtime, which interferes with the smooth operation of the fleet. These structural inspections need to be very frequent, since the remaining members can fail shortly after the failure of the primary member. At present, there seem to be a lack of rational methods available to assess the reliability of a fail-safe design as a function of the selected inspection interval.

A computer simulation program, ***Fail-Safe***, has been written to simulate a dual-path, discrete member fail-safe design. The lives to failure are simulated by a two-parameter Weibull distribution while the service life to retirement is simulated by a normal distribution. It is assumed that each inspection serves to determine whether *both* load paths are intact, and that these inspections are 100% reliable. Inspection threshold and inspection intervals are selected by the ***Fail-Safe*** operator. The computer program performs a large number of simulations and determines for each simulation: (1) Has the aircraft retired from service with both members intact? (2) Has one member failed but the failure was detected prior to the second failure? (3) Has a total (catastrophic) failure occurred? From the statistical results of more than 80,000 simulations, the computer program determines the probability of total failure. The program operator can then modify the inspection threshold and inspection interval until the required reliability is achieved.

A series of parametric studies were performed using ***Fail-Safe***, accounting for such variables as: inspection threshold, inspection interval, aircraft aging, the effect of materials used and the ratio of secondary to primary member fatigue life. Each parametric study resulted in a calculation of the probability of total failure.

Based on these studies, recommendations are given concerning inspection thresholds and intervals, preferred materials and optimized ratios of fatigue lives. These recommendations will allow the design of a fail-safe system having rationally determined inspection thresholds and intervals. Figure 3 shows a typical result of a fail-safe study with the probability of total failure shown as a function of the inspection interval.

The results of this investigation are summarized in [15] and will be presented at the 21st ICAF Symposium.

11.3.2 Failure of Adhesively Bonded Joints (V. Weissberg et al, IAI)

Cracked structures generally fail either in a net-section failure mode or when the stress intensity exceeds the fracture toughness of the material. The stress intensity of a bonded joint is shown to be proportional to square-root of the bond thickness, thereby insuring that numerically it will be quite low. It is also shown, by finite-element model studies, that the stress intensity of a bonded joint and its stress concentration factor are linearly related. An experimental program was performed for double cantilever beam, end notch flexural and mixed mode flexural specimens, in which the specimens were loaded to failure. In all cases, the failures occurred at stress values exceeding the yield strength of the adhesive. This demonstrated that the mode of failure is dictated by the net-section properties of the adhesive and not by its fracture toughness. It was also concluded that a cracking failure could only occur if the surface preparation was not performed correctly and the adherend to adhesive interface was weak [16].

11.3.3 Failure Criteria for Singular Points in a Brittle Elastic Material (G. Amar and Z. Yosibash, Ben-Gurion University)

A research project partially reported in [17] is directed towards the solutions of linear elastostatic problems in the vicinity of reentrant corners, or multi-material interfaces, and the formulation of a failure criterion for these problems. The theory of fracture mechanics, applicable to cracked domains is only a small restricted part of a more *general approach for predicting failure initiation* in structural components subject to mechanical or thermal loading, which is being developed by an analytical, numerical and experimental approach. Realistic examples of such failures range from an electronic chip (failure at reentrant corner due to temperature loading), to larger components such as a reentrant corner in a structural PMMA (Perspex) part having a V-notch. Figure 4 shows the actual failure of an electronic chip and a p-version finite-element analysis of the failure zone. Figure 5 describes a V-notch failure analyzed by this technique.

This investigation, which is performed in collaboration with Dr. A. Busiba from the Material Engineering Department at Ben-Gurion University, is aimed at the formulation of a robust failure criterion which would provide the ability to predict failure initiation at singular points in a brittle elastic material based on the specific geometry, material properties and loading. It is aimed at providing the tools to prevent these failures by proper design. The analytical-numerical tool is used for extracting the quantities representing the elastic field in the neighborhood of any singular point, based on a generalized failure mechanics theory in conjunction with the p-version finite element method. This information enables the computation of the elastic strain energy density, which is proposed as a failure criterion. This criterion should be applicable to any notch angle in brittle materials.

The approach has been compared to some experimental results found in a paper by Dunn [33] for a three-point V-notched specimen and preliminary results with PMMA specimens tested by Dr. Busiba. A FE analysis of a 3-point bending specimen was built, simulating the experiments done by Dunn [34]. Tests on alumina (Al_2O_3) notched specimens (Figure 6), having various notch angles, are underway in order to evaluate the applicability of the proposed failure criterion.

11.3.4 Interface Fracture of Isotropic and Transversely Isotropic Materials (L. B. Sills et al, Tel-Aviv University)

In continuation of an activity that was presented in the previous National Review [1], an investigation was conducted to determine the behavior of cracks along an interface between isotropic materials and a pair of transversely isotropic materials. A methodology was developed to measure the interface fracture toughness using *Brazilian disk specimens.* Two pairs of isotropic materials were considered: glass/epoxy [18] and a ceramic pair (K142/K144) [19]. Stress-intensities were determined using finite-elements and the conservative M-integral. The effect of residual stresses was accounted for by the use of a weight function. The total stress-intensity was obtained by superposition. The results were compared to the results obtained from the glass/epoxy specimens [20]. The work was later extended to consider the delamination of a laminated composite [21].

11.4 AIRCRAFT PROJECTS

11.4.1 Galaxy Executive Jet Fatigue Substantiation Program (S. Afnaim and A. Brot, IAI)

The Galaxy, wide-body executive jet received its type certificates from the CAA of Israel and the FAA in December 1998. The Galaxy has a transatlantic range and a maximum cruise speed of Mach 0.85. It can transport up to 18 passengers in a corporate configuration and up to nine passengers in an executive configuration. The Galaxy is powered by two PW306A jet engines. The Galaxy primary structure is metallic except for the ailerons, elevators and rudder that are manufactured from composite materials.

The Galaxy airframe structure has been substantiated to the FAR-25 damage-tolerance requirements. In addition, fatigue and damage-tolerance component and full-scale tests are being performed in order to support the damage-tolerance analyses. Several of these tests were described in the 1999 National Review [1]. This review describes activities performed since 1999. Reference [22] and [23] describe in detail the damage tolerance substantiation of the Galaxy Executive Jet as well as the fatigue testing program.

11.4.1.1 Full-Scale Fatigue Test

The Galaxy has been designed to a service life objective of 36,000 hours and 20,000 flight cycles. In order to substantiate this life objective, the aircraft is being tested in a full-scale fatigue test for a duration of two lifetimes.

The test-article for the full-scale fatigue test consists of all the structural members of the fuselage and both wings. The empennage is being fatigue tested separately. The test aircraft was mounted to the test fixture at the nose landing gear attachment and at the engine mount fittings. Figure 7 is a photo of the Galaxy aircraft mounted in its loading fixture.

The fatigue spectrum loading consists of randomly selected flight-by-flight sequences, reflecting the anticipated usage of the aircraft. A flight consists of the various flight and ground events that the aircraft will experience. Approximately 20 events per flight have been included in the 2000 flight spectrum block.

The test-article was divided into 29 loading zones, each of which is independently loaded during each event of the spectrum, using 42 servo-hydraulic actuators. In addition, the passenger cabin and baggage compartment is pressurized, using compressed-air during the airborne events of the spectrum. The zone loading for each event was determined using a "constrained least-square error method" which minimized deviations in loading of the important structural parameters. Approximately 800 strain-gages have been bonded to the test-article, mainly to monitor the onset of cracking.

Testing began in December 1998 and has reached 25,400 flights by the end of March 2001. The aim of the test is to reach two lifetimes (40,000 flights equivalent to 72,000 flight hours) of fatigue cycling. Strains are monitored every 500 flights; whenever a large deviation in strains is observed, the area is inspected for cracks. NDI is performed at 2500 flight intervals.

A number of cracks have been detected during the full-scale test, in the following areas:

- Baggage compartment
- Nose landing gear bay in the forward fuselage
- Cabin forward and aft pressure bulkheads
- Windshield sill beam
- Wing lower skin, at Rib 2

In all cases, the crack growth rates were sufficiently slow, as not to result in any danger. Nevertheless, design changes were introduced to improve the durability of the structure in all these areas. These design changes were introduced in new production and will be retrofitted to the existing fleet. Strain levels were measured in the region of the design changes and, in all cases, were found to be sufficiently low to insure an adequate fatigue life.

At the 22,500 flight inspection, a crack was detected on the RHS wing lower skin, at the intersection of Rib 2 and the Main Landing gear bay. At the time of detection, the crack had a length of approximately 25mm, reaching the edge of the skin. Fractographic analysis of the crack indicated that the crack grew for more than 10,000 flights before reaching a length of 25mm. This demonstrated the damage-tolerance capability of this wing location.

The cracking was caused by a fillet of insufficient radius (sharp edge) which was introduced at a skin thickness step of the RHS test wing. The LHS wing had a radius of 5 mm at the same location and no cracking was detected. A detailed finite-element model confirmed the high stresses in the area of the skin thickness step. On the RHS wing, the cracked material has been removed and a composite material patch was bonded on the lower skin to allow it to complete the test. (The patch consists of 26 layers of carbon-epoxy, applied by wet lay-up, and post-cured after installation.) The test resumed following the bonding of the patch, after confirming that the stress levels of the wing under the patch have been reduced significantly. Figure 8 is a photograph of the composite material patch that was bonded to the test wing lower skin.

An independent test program will be performed in order to study the fatigue characteristics of this cracked location and to evaluate various reinforcement schemes. Two lower wing lower skin components, simulating the Rib2 area, will be tested with initial flaws introduced at the most critical locations. Spectrum loading will be applied during the test and a residual strength load will be applied at the end of the component test.

11.4.1.2 Empennage Fatigue and Damage-Tolerance Test:

The entire empennage assembly has been mounted to an aft fuselage structure for fatigue testing, as is shown in Figure 9. The test includes the elevator and rudder, which have been manufactured from composite materials. The loading spectrum includes vertical and lateral loading resulting from gust and maneuvers as well as measured buffeting loads arising from thrust reverser deployment. The horizontal and vertical tails were divided into ten loading zones, each of which is independently loaded during each event of the spectrum, using servo-hydraulic actuators. Approximately 200 strain-gages were bonded to the structure for strain monitoring, which is performed every 1000 flights. The test-article is inspected for cracks at 5000 flight intervals.

The composite material elevator and rudder will be tested for damage-tolerance under manufacturing and service-inflicted damage as well as under barely-visible impact damage.

The Galaxy Empennage test, that started in December 1998, has reached one lifetime (20,000 flights) of testing. The aim of the test is to reach two lifetimes of fatigue testing followed by one lifetime of damage-tolerance testing (total of 60,000 flights), as was described in the ICAF 1999 National review [1].

At 10,000 flights, strain-gages located on the horizontal stabilizer rear spar began to show slight changes. The horizontal stabilizer was disassembled during the 20,000 flight inspection, and it was discovered that cracking had initiated at several of the fastener holes connecting the pickup fittings to the rear spar web. The fact that the cracks grew for more than 10,000 flights without resulting in failure, demonstrated that the location is damage-tolerant.

Flight testing of a Galaxy aircraft, together with customer surveys on similar aircraft has disclosed that the engine reverse thrust buffeting loads that were used in the empennage fatigue test were overly severe. The test loading spectrum has been altered and a less severe spectrum, taking into consideration the more frequent usage of "idle" engine reverse thrust, is being applied for the continuation of the test. Figure 10 describes a typical time-history of the asymmetric strains on the horizontal tail during maximum reverse thrust application, as measured during flight testing of a Galaxy aircraft.

11.4.1.3 Main Landing-Gear Fatigue Test

The main landing gear spectrum loads are applied in the vertical, drag and side directions on the Galaxy landing gear. A truncated fatigue-load spectrum of the ground-loads is used for this test, after combining and simplifying some of the ground-operations. Each flight-cycle consists of taxi, turning, braking, pivoting, rotation and landing-impact events. The test spectrum was truncated to include approximately 20 events per flight. Groups of 1,000 of these flights were assembled into each block of flight-cycles for the fatigue-test load-spectrum.

The Galaxy landing gear is being fatigue tested to five lifetimes. By the end of March 2001, the main-gear has exceeded 76,000 flights with no significant failures or detectable damage.

11.4.2 Low-Altitude Operation of an Astra SPX Aircraft (S. Afnaim and A. Brot, IAI)

An Astra SPX executive jet aircraft has been substantiated for *special usage*, including the installation of equipment pods under the wings.

From fatigue considerations, the main change is the usage of the aircraft. The aircraft will be used mainly in this *special usage* role (60% of missions); the remaining missions (40%) will be similar to the typical high-altitude Astra missions. The *special usage* missions will be performed at an altitude of 5,000 ft where the aircraft is subjected to a severe fatigue gust spectrum. A special spectrum for this type of operation has been generated; it is compared to the typical Astra SPX spectrum in Figure 11.

The damage-tolerance analysis of all points influenced by the change has been repeated and the inspection intervals, appropriate to the specific usage, have been determined. The results show a significant reduction in inspection intervals from the original maintenance schedules.

11.4.3 A Damage-Tolerance Approach for Life Extension of a Helicopter Pitch-Housing (M. Ben-Noon, IAF)

The pitch-housing component in the IAF AH-64A Apache helicopter (Figure 12) is currently replaced by the IAF at specific intervals, based on the "safe life" replacement policy recommended by the manufacturer. This policy was thought to be unnecessarily conservative and costly. An investigation to extend the service life of the 7049-T73 aluminum pitch-housing by using an "on-condition" replacement procedure was performed. Up to now, no pitch housing removed from IAF aircraft has exhibited fatigue cracks.

Spectrum evaluation and crack growth analysis of the pitch-housing lug was performed in order to determine whether the component has the potential to be used safely for additional flight hours by inspecting periodically for cracks. This analysis was performed using NASTRAN/PATRAN and Stress-Check finite-element software and NASA/FLAGRO crack growth software. The loading spectrum was based on cycle count data taken from flight tests. The analysis had to deal with the effects of large compressive stresses in the lug as well as the effect of an interference-fit bushing. Stress-intensities in the lug were calculated using the Stress-Check p-version finite-element software. External loads, as well as stresses induced by the interference-fit bushing, were accounted for in the calculation of the stress-intensity factors. Crack growth analysis was performed, accounting for a salt-fog working environment.

A three-stage test program is presently underway in order to verify the analytical results. Specimen tests are being used to confirm the crack growth material properties. Spectrum tests on pitch-housing lug specimens will be used to verify the crack growth analysis. Pitch-housings, removed from service after 2,000 flight hours, will be tested to assess their remaining life.

A final decision on implementing this life extension program on the IAF fleet awaits the results of these on-going flight spectrum tests, and the development of adequate NDI techniques. A summary of this investigation is contained in [24].

11.5 COMPOSITE MATERIALS

11.5.1 COMPRES: A Multi-National EU Funded R&D Project for Bonded Composite Repairs (A. Nathan, IAI)

This program for composite material repair of aging commercial aircraft was presented in the 1999 ICAF National Review [1]. The program was then just at its inception, and thus the review only included a list of the consortium partners, objectives of the project and a list of proposed tasks. A short synopsis of these topics will be included here, and then an emphasis will be placed on work completed to date in the project.

The objective of the project is to produce a methodology for standardized composite material bonded repairs of metallic structure for aging commercial aircraft. IAI serves as the technical coordinator of this Brite Euram 4th framework project. HAI of Greece is in charge of overall management. The consortium make-up includes the necessary ingredients for a successful project. Aircraft manufacturers, maintenance facilities, composite material suppliers, repair equipment manufactures, universities and research institutes from France, England, Italy, Portugal, Israel and Greece are all involved in the project.

Bonded composite repairs have a number of advantages over the metallic fastened repair, including uniform and efficient load paths, elimination of fastener holes/stress concentrations, good fatigue characteristics and corrosion resistance, etc. Bonded composite repairs have found many military applications over the past 20 years, for example, the F-111 wing pivots, C-141 wing skins, C-130 wing stiffeners, the B1 dorsal longeron, and the repair of Mirage and Kfir lower wing skins. Today we are finding a greater awareness in the commercial arena, for example, with the boron-epoxy doubler repair of the L-1011 door corner.

The following tasks have made significant progress or have already been completed:

- Statistical study of primary structures prone to damage
- Comparison of optimum analysis methods to analyze composite material repairs
- Extensive testing of composite material systems for repairs
- Development of low energy curing cycle to minimize residual thermal mismatch stresses
- Parametric analysis of real structures to be included in the repair manual
- Round-robin study of optimum surface treatment method
- Development of innovative phosphoric acid anodize closed loop field service equipment
- Innovation induction heating technology to reduce residual thermal mismatch stresses
- Round-robin study of optimum NDE method to detect disbonds, delaminations and cracks beneath the patch
- Comprehensive coupon, element and component testing has been initiated

Figure 13 describes a p-version finite-element analysis of a skin to frame attachment, including the existence of a crack by a fastener hole. This analysis was performed during the COMPRES Program in support of designing a composite repair of a cracked structure.

Advances in the state-of-the-art of bonded composite repairs have been accomplished or are expected. Some examples include:

- Repair manual for "characteristic structure"
- A large emphasis on helping reduce the detrimental residual stresses caused by thermal mismatch between composite material and metallic parent structure. This has been attacked by lower energy cure cycles, induction heating for curing adhesive and patch, as well as analytical support.
- Improved surface preparation equipment
- 3D, parametric, p-version finite element analysis of bonded repair

This program is now in its final year and the repair manual for *characteristic structures* is expected to be released in early 2002.

11.5.2 Bonded Composite Repair of Metallic Structures (I. Kressel, IAI)

Bonded composite repairs for metallic aircraft structures must carry the required design loads under hostile environmental conditions, including a temperature range from -54°C up to 70°C.

Advanced composite materials such as carbon/epoxy or boron/epoxy have a very low coefficient of thermal expansion in the fiber direction, with respect to the mating aluminum structure. Since the bonding and curing of a composite patch usually requires elevated temperature, thermal residual stresses may develop. These residual thermal stresses have an adverse effect on the fatigue performance of the composite patch, since tension stresses are induced in the repaired aluminum structure.

Two aspects of the thermal mismatch were considered:

1. Analytical estimation of residual stresses due to the entire cure cycle.
2. Development of an analytical method for crack growth calculation for bonded repairs.

11.5.2.1 Thermal Expansion Mismatch in Bonded Composite Repairs

The cure cycle is a three-step process:

- **Heating phase:** the repaired structure is heated but no structural connection exists between the patch and the aluminum structure**.**
- **Curing phase:** the adhesive is cured at a constant temperature for an allocated time
- **Cooling phase:** the repaired structure is cooled down to room temperature. In this stage the repaired structure and the patch are bonded together

The cure cycle is analytically approximated as a two-step process. The curing phase is ignored since no additional stresses develop in this phase. The residual stresses caused by the cure cycle can be calculated as a linear combination of two solutions:

- Analysis of the metal structure to simulate the heating phase.
- Analysis of the repaired structure (including adhesive and patch) to simulate the cooling to room temperature phase.

This process is shown schematically in Figure 14.

11.5.2.2 Crack Growth Analysis of the Metallic Structure

An analysis was performed, using the Walker crack growth model, to predict fatigue crack growth of a metallic structure that has been repaired with a composite patch. The loading included the applied stresses as well as the thermal residual stresses that were induced by the temperature mismatch.

A p-version (NASTRAN) finite-element model was generated in order to determine the stress-intensity of the crack. The model contained the metal plate, the adhesive and the composite patch. The stress-intensity factor was calculated using the energy release method. The results of the analysis are presented in Figure 15. The results indicate that the patch efficiency is increased as the crack length is increased. The results of this analysis can be used to assess the effectiveness of a composite repair on an aircraft structure.

11.5.3 Damage Detection in Composites (P. Pevzner, T. Weller and A. Berkovits, Technion)

A new approach for damage detection in composite materials has been developed. Optic fibers, that were stripped of their jackets and weakened, were embedded in a composite structure in a manner that caused them to crack in the presence of cracks and delaminations in the composite. It was shown that, at the location of a crack in a fiber, transmitted light energy was converted into heat energy, causing the temperature in the region of the crack to rise. The temperature change was detected by an infrared camera.

Dynamic numerical simulations of the heating in the neighborhood of the fiber crack were performed. An analytical solution of the temperature distribution on the surface of a composite plate above a crack was also developed. Both the analytical and numerical results showed the feasibility of detecting and monitoring the hot-spot on the composite plate by using an infrared camera. An experiment was conducted that confirmed the feasibility of the concept. The effect of fiber depth, heat conductivity and light power on the temperature distribution was also investigated. The findings are expected to be published in the near future.

11.5 LOADING SPECTRA DEVELOPMENT

11.6.1 Nose Landing Gear Taxiing Loads (A. Brot and D. Chester, IAI)

Several references exist in the technical literature describing the vertical load-factor excursions (Δn_z) at an aircraft center-of-gravity (c.g.) while taxiing over a runway. But none of these references contain data relating the nose landing gear load reactions to the aircraft c.g. load-factors. Some aircraft manufacturers, when generating a nose landing gear loading spectrum, made the *simplifying* assumption that the nose gear reaction excursions, normalized to the nose gear static reaction, will be equal to the load-factor excursions at the aircraft c.g. This simplifying assumption has been shown to be *extremely unconservative*.

Buxbaum presented measured Airbus A-300 taxi test data showing that, in fact, the nose landing gear vertical load excursions are 2 – 3 times larger than those at the main landing gear [25].

Chester developed analytical expressions that confirmed Buxbaum's measured test data and explained that the above magnification factors result from the interaction between aircraft pitching and heaving motions when encountering an obstacle [26]. Further studies of this phenomenon, as experienced during landing-impact, have been reported in two additional technical papers written by Chester [27] and [28].

The present investigation utilizes a computer simulation of a rigid aircraft having flexible nose and main landing gears. The aircraft is allowed to taxi, at various forward speeds, on a representative runway having a random profile. The load-factor excursions at the c.g. and at the main and nose landing gears are determined by the simulation.

A typical medium sized aircraft was defined from the standpoint of geometry, landing gear properties and mass and inertia properties. Simulations at various forward velocities for randomly varying runway profiles were performed, and the results were presented. The results indicate how the nose gear load magnification factor varies with the range of parameters that have been considered. Simulation studies have confirmed this phenomenon, first described by Buxbaum and Chester, that nose-gear load excursions during taxiing are generally 2—3 times larger than those at the aircraft center-of-gravity. Figure 16 describes the results of a simulated ten-second taxi sequence at a speed of 40 knots. The time-history of the main and nose landing gear loads, normalized to their static reactions, is shown. The runway profile is also plotted against the time that the *nose landing gear* passes over each bump. Figure 16 clearly shows that the nose landing gear vertical load excursions are 2 – 3 times larger than those at the main landing gear.

Simulation results can be expected to provide useful data for generating realistic nose landing gear spectra. The results of this study were presented at the ASIP 2000 Conference [29].

11.6.2 A Parametric Study of Aircraft Landing Impact (D. Chester, IAI)

A parametric approach to the simulation of aircraft landing impact has been used, with pitching and heaving degrees of freedom. The simulation determines the response of main and nose landing gears, arranged in the usual tricycle layout.

The following external conditions were varied as independent quantities: tail-down angle, sinking-speed, pitching moment-of-inertia and aircraft size. Compared to the independent landing-gear behavior that is usually assumed, when these aircraft motions are included, there are important differences in each gear's landing conditions and in the resulting vertical loads and displacements.

For the two main-gears, the maximum vertical loads are almost linearly dependent on the sinking-speed, but there is some variation in the proportion of kinetic energy absorbed with variation of the other three aircraft parameters. For the nose-gears no similarity exists compared to what is often assumed for the single gear. In particular correlation with aircraft sinking-speed is absent. However the response is strongly affected by the variation in the values of initial pitch angle, pitch inertia and the aircraft scale. This is expressed by the variation of the equivalent mass fraction at this location.

Figure 17 describes the variation of nose landing gear parameters with the initial tail-down angle. The results of this investigation were presented at a recent ICAS Congress [28].

11.7 COMPUTATIONAL METHODS

11.7.1 Singular Solutions Caused by Edges, Vertices or Abrupt Changes (Z. Yosibash, Ben-Gurion University)

This investigation, presented in [30] deals with numerical methods for computing singular solutions of linear second-order elliptic partial differential equations (Laplace and Elasticity problems) in polyhedral domains. The singularities may be caused by edges, vertices, or abrupt changes in material properties or boundary conditions. In the vicinity of the singular lines or points the solution can be represented by an asymptotic series, composed of eigen-pairs and their amplitudes. These are of great interest from the point of view of failure initiation because failure theories directly or indirectly involve them. The paper addresses a general method based on the modified Steklov formulation for computing the eigen-pairs and a dual weak formulation for extracting the amplitudes numerically using the p-version of the finite element method. The methods are post-solution operations on the finite element solution vector and have been shown in a two dimensional setting to be super-convergent.

11.7.2 An Adaptive Finite-Element Program for Crack Growth (D. Givoli, Technion)

A new crack growth computer program, based on finite-elements (FE), is being developed. This program combines the relative simplicity of crack growth computation with the generality and accuracy of a full FE analysis. The program is based on linear elastic fracture mechanics (LEFM) principles combined with FE mesh adaptation techniques.

Crack growth analysis in the aerospace industry is usually performed, subject to several assumptions: (1) it is assumed that the geometry and loading are sufficiently simple so that the stress-intensity solution can be defined by an analytical or empirical expression. (2) It is frequently assumed that the loading and geometry give rise to a pure Mode I problem. (3) It is usually assumed that, in a Mode I dominated case, the crack extends in a straight line perpendicular to the remote tensile load. Under these assumptions, the analysis is straightforward.

On the other end of the spectrum, detailed two or three-dimensional finite-element models are sometimes built for very critical cases where high accuracy is required for complex loading or geometry.

There have been several attempts to combine FE models with a crack growth analysis. Most of these methods are still subject to assumptions (2) and (3). This program deals with the general case of mixed-mode crack behavior along a crack path that has not been predetermined. The program, which is highly automated, is based on the use of a standard FE code. At present, the program is limited to two-dimensional geometry but will, in the future, be extended to three-dimensional geometries. The program, which is based on LEFM, operates according to the following steps:

A. Mesh generation for the uncracked model
B. FE analysis of the uncracked model
C. Introduction of an initial crack
D. Update of the geometrical model
E. Mesh generation and refinement
F. FE analysis of the cracked model
G. Calculation of the energy release rate and stress-intensity factor
H. Checking for unstable growth

I. Checking for crack closure
J. Checking for crack reaching a boundary
K. Calculation of crack propagation rate
L. Calculation of the crack growth direction (two stress and one displacement criteria)
M. Going on to the next iteration (step C)

Several two-dimensional numerical examples were performed, which compared favorably to experimental results. Figure 18 shows the calculated solution for the problem of a *crack approaching a hole*. The curved crack path is evident. The method has been applied to other problems such as a *beam under an oscillatory force* and *fatigue cracking of a gear tooth*.

Results of this investigation have been published in [31] and [32].

11.8 MISCELLANEOUS

11.8.1 N.D.E Methods for Corrosion Detection (U. Sol, IAI)

In recent years, IAI has been involved in the development and refinement of NDE methods. An experimental investigation was performed on specimens containing pitting and exfoliation corrosion. This investigation was aimed at determining the comparative ability of various NDE systems to detect hidden-corrosion. The NDE systems tested included conventional radiographic and eddy-current methods, as well as more advanced methods such as magneto-optic, ComScan and MWM (Meandering Winding Magnetometer). The investigation included an assessment of these methods, a comparison of their ability to detect and estimate the severity of corrosion, their ability to inspect large areas as well as relative costs. IAI has also developed an "*expert NDE system*" which includes a fuzzy-logic knowledge based system to detect, assess and categorize damage. The system is designed to distinguish between hidden-corrosion and artifacts.

11.8.2 Further Modification of the Bolotin Method in Vibration Analysis (P. Pevzner, T. Weller and A. Berkovits, Technion)

The Bolotin method (BM) or the modified Bolotin method (MBM) are often used to determine natural frequencies and mode shapes of isotropic and orthotropic rectangular plates. Unlike these methods, the present approach does not postulate the formula for eigenfrequency, but rather is based on the condition that the frequency obtained from the governing differential equations has to be equal to that yielded by the Rayleigh method. This modification is shown to be more straightforward and faster in computation, and the derived mode shapes are valid on a larger portion of the plate. Furthermore, the proposed modification easily provides a solution for boundary conditions for which the BM and MBM cannot provide a solution. Problems with two different sets of boundary conditions were solved in this study: a rectangular orthotropic plate with all edges clamped and rectangular isotropic and orthotropic plates clamped along one pair of opposite edges and free along the other pair. The results obtained for the first set compared favorably with those yielded by the MBM and Rayleigh methods, In the second case, the BM and MBM method failed to predict the beam-like modes of vibration, while the present modification treats the problem satisfactorily [33].

11.9 REFERENCES

1. Berkovits, A., "Review of Aeronautical Fatigue Investigations in Israel, April 1999 – March 2001", *Minutes of the 26th ICAF Conference*, Bellevue, Washington, USA, 1999.

2. Tirosh, J. and Peles, S., "Bounds on the Fatigue Threshold in Metals", *Journal of the Mechanics and Physics of Solids*, Elsevier Science Ltd., 2001.

3. Konstantino, E. and Altus, E., "Fatigue Life Enhancement by Laser Surface Treatment", *Surface Engineering,* 15(2), 1999.

4. Altus, E., and Konstantino, E., "Optimum Laser Surface Treatment of Fatigue Damaged Ti-6Al-4V Alloy", *Materials Science and Engineering,* A302, 2001.

5. Peles, S. and Weiss, M., "A Modified Two-Term Fatigue Life Prediction Model for Mean Stresses in Steel", *Proceedings of the Fatigue '99 Conference,* 1999.

6. Peles, S., "Development of a Multi-Term Relation for Prediction of Fatigue Crack Propagation in Metals", Ph.D. Research Thesis, Technion – Israel Institute of Technology, 2000.

7. Weiss, M., and Peles, S., "Extension of the Two-Term Fatigue Model for Mean Stresses and for the Crack Closure Effect", Submitted to: *The International Journal of Fatigue,* 2001.

8. Peles, S. and Weiss, M., "Analytic Considerations and Validation of the Two-Term Fatigue Model", Submitted to: *The International Journal of Fatigue,* 2001.

9. Perl, M., "An Improved Split-Ring Method for Measuring the Level of Autofrettage in Thick-Walled Cylinders", *Journal of Pressure Vessel Technology,* ASME, Vol. 120, February 1998.

10. Perl, M., Levy, C and Bu, J., "Three-Dimensional Analysis of a Semi-Elliptical Crack Emanating from an Erosion at the Bore of an Autofrettaged Pressurized Cylinder", *Journal of Pressure Vessel Technology,* ASME, Vol. 121, May 1999.

11. Perl, M., and Greenberg, Y., "Three-Dimensional Analysis of Thermal Shock Effect on Inner Semi-Elliptical Surface Cracks in a Cylindrical Pressure Vessel", *International Journal of Fracture,* Vol. 99, 1999.

12. Perl, M., "The Change in Overstrain Level Resulting From Machining of an Autofrettaged Thick-Walled Cylinder", *Journal of Pressure Vessel Technology,* ASME, Vol. 122, February 2000.

13. Perl, M. and Nachum, A., "3-D Stress Intensity Factors for Internal Cracks in an Overstrained Cylindrical Pressure Vessel – Part I: The Effect of Autofrettage Level", *Journal of Pressure Vessel Technology,* ASME, Vol. 122, November 2000.

14. Banks-Sills, L. and Eliasi, R., "Fatigue Life of a Cannon Barrel", *Engineering Failure Analysis,* Vol. 6, 1999.

15. Brot, A. "Assessing the Reliability of Fail-Safe Structures", to be presented at the 21st ICAF Symposium, June 2001.

16. Weissberg, V. et al, "Crack Propagation vs. Yielding in Adhesively Bonded Joints", *Proceedings of the 41st Israel Annual Conference on Aerospace Sciences,* 2001.

17. Amar, G. and Yosibash, Z., "P-FEM for Formulating an Elastic Criterion for Predicting Mechanical Failures at 2-D Singular Points", *P-FEM 2000 Conference Proceedings,* 2000.

18. Banks-Sills, L. et al, "A Methodology for Measuring Interface Fracture Properties of Composite Materials", *International Journal of Fracture,* **99** (1999) 143-161.

19. Banks-Sills, L. et al, "Interface Fracture Properties of a Bimaterial Ceramic Composite", *Mechanics of Materials,* 32, (2000), 711-722.

20. Banks-Sills, L. and Ashkenazi, D., "A note on Fracture Criteria for Interface Fracture", *International Journal of Fracture,* **103** (2000), 177-188.

21. Banks-Sills, L. and Boniface, V., "Fracture Mechanics for an Interface Crack between a Special Pair of Transversely Isotropic Materials", to appear in *Multi-scale Deformation and Fracture in Materials and Structures – The James R. Rice 60th Anniversary Volume.*

22. Brot, A., Afnaim, S. and Granot, Z., "Damage Tolerance Substantiation of the Galaxy Executive Jet", *Proceedings of the 20th ICAF Symposium,* 1999.

23. Brot, A., Afnaim, S. and Granot, Z., "Fatigue and Damage Tolerance Testing of the Galaxy Executive Jet", *Proceedings of the 40th Israel Annual Conference on Aerospace Sciences,* 2000.

24. Alon, L., et al, "A Damage-Tolerance Approach for Life Extension of a Dynamic Component", *Proceedings of the 41st Israel Annual Conference on Aerospace Sciences,* 2001.

25. Buxbaum. O., "Landing Loads of Civil Transport Airplanes", *8th Plantema Memorial Lecture, Proceedings of the 11th Symposium of the International Committee for Aeronautical Fatigue (ICAF)*, Noordwijkerhout, Netherlands, 1981.

26. Chester, D. H., "The Equivalent Masses at Nose Landing Gears During Landing Impacts and When Taxiing Over Runway Perturbations", *Israel Journal of Technology, Vol. 23,* 1986.

27. Chester, D. H., and Brot A., "Development of a Fatigue Spectrum for the Nose Landing Gear of the Galaxy Executive Jet", *Proceedings of the 26th Symposium of the International Committee for Aeronautical Fatigue (ICAF),* Seattle, 1999.

28. Chester, D. H., "A Parametric Study of Aircraft Landing Impact, With Emphasis on Nose Landing Gear Conditions", *Proceedings of the 22nd International Congress of Aeronautical Sciences (ICAS),* Harrogate, UK, 2000.

29. Brot, A., and Chester, D., "Determining Nose Landing Gear Taxiing Loads by Computer Simulation", *Proceedings of the 2000 USAF Aircraft Structural Integrity Program* Conference, 2000.

30. Yosibash, Z., "Computing Singular Solutions of Elliptic Boundary Value Problems in Polyhedral Domains Using the P-FEM", *Applied Numerical Mathematics*, **33**, pp. 71-93, 2000.

31. Givoli, D. and Zusman, R., "An Adaptive Finite Element Framework for Fatigue Crack Propagation", *Proceedings of the 22nd International Congress of Aeronautical Sciences (ICAS),* Harrogate, UK, 2000.

32. Givoli, D. and Zusman, R., "An Adaptive Finite Element Framework for Fatigue Crack Propagation", *(has been submitted to the International Journal of Numerical Methods in Engineering), 2001.*

33. Pevzner, P., et al "Further Modification of Bolotin Method in Vibration Analysis of Rectangular Plates", *AIAA Journal,* Vol 38, No. 9, 2000.

34. Dunn M. L., et al, "Fracture Initiation at Sharp Notches: Correlation Using Critical Stress Intensities", *International Journal of Solid Structures*, 34(29), 3873-3883, 1997.

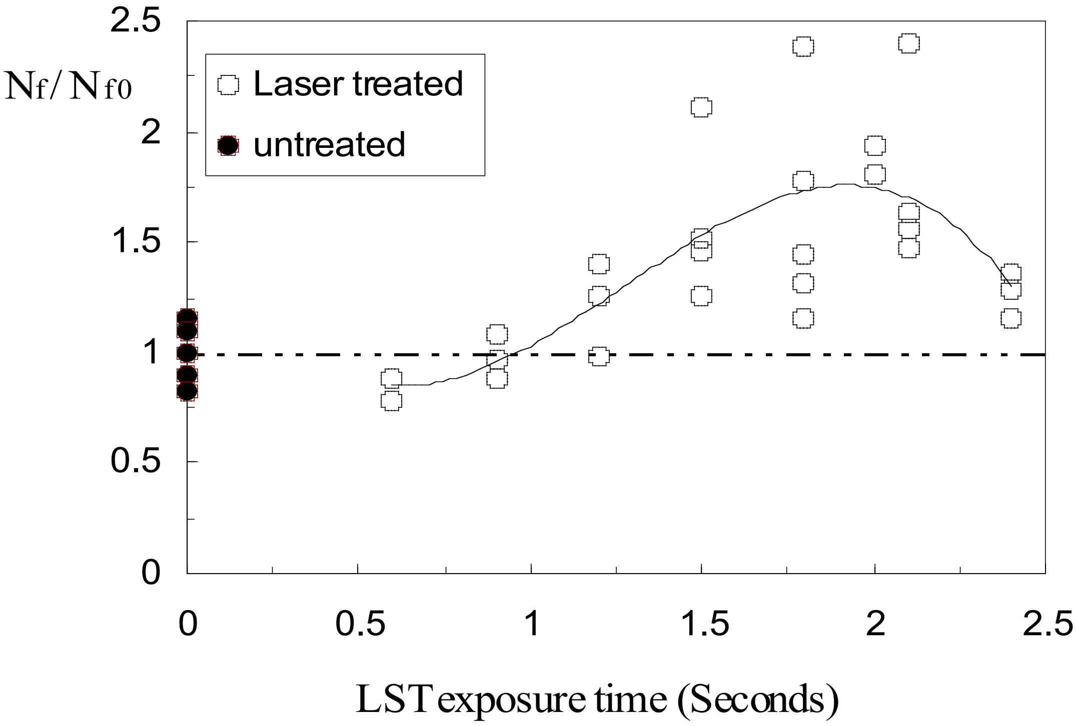

Figure 1: Effect of Laser Surface Treatment (LST) Exposure Time on Fatigue Life

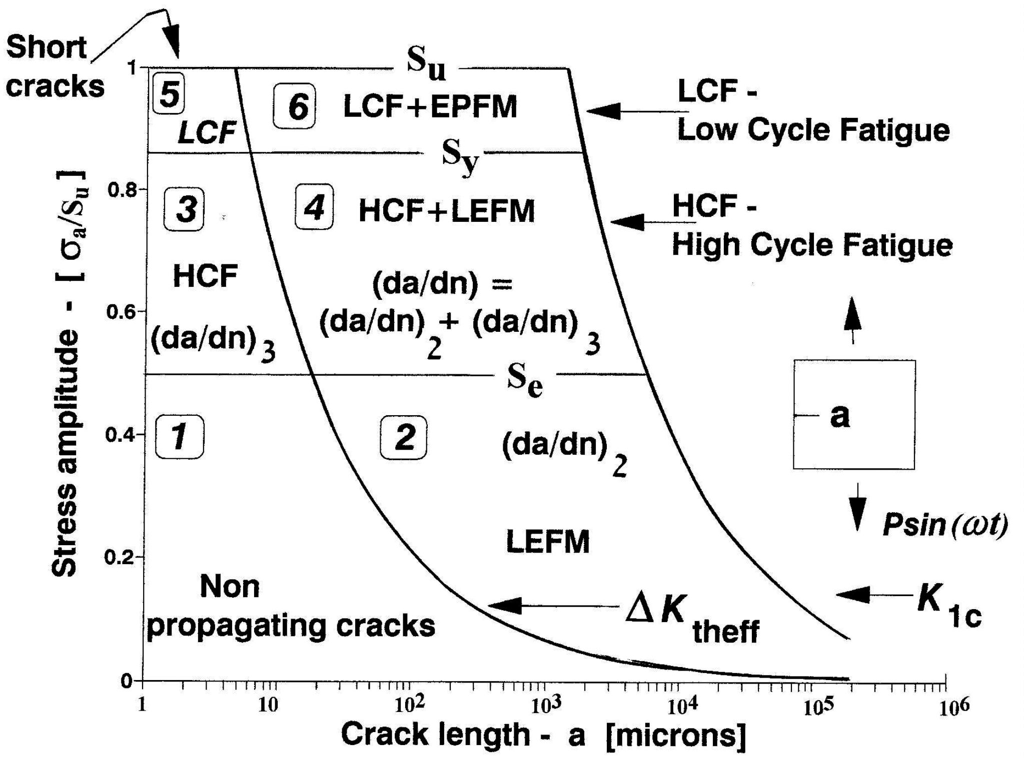

Figure 2: **Fatigue Domain Divided into Fatigue and Fracture Regimes and Six Zones**

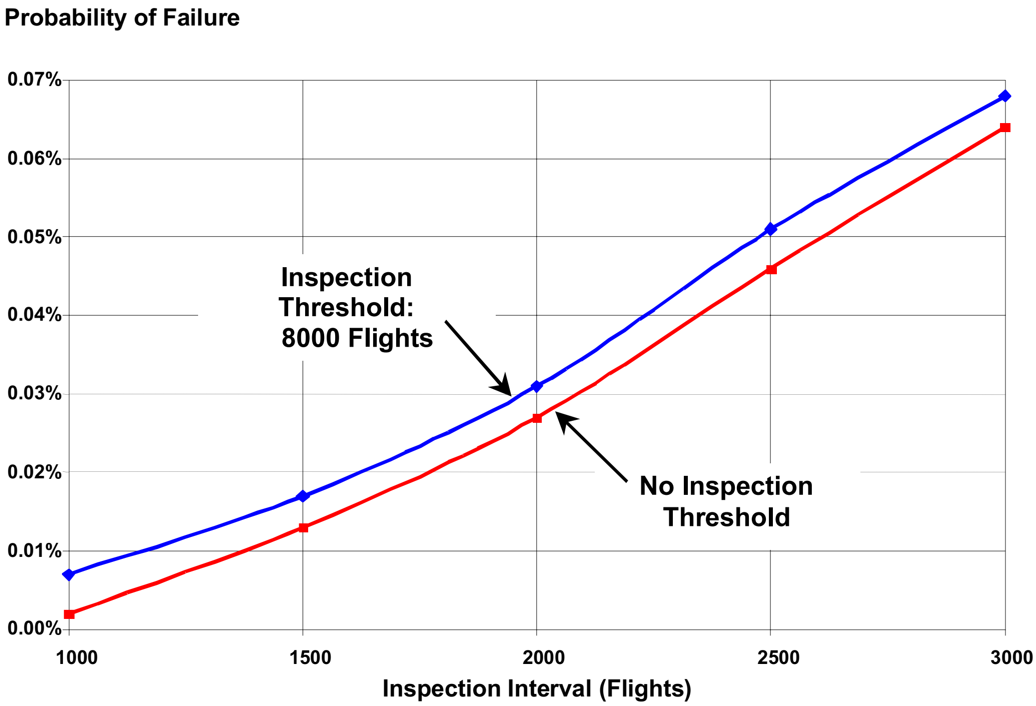

Figure 3: Effect of Inspection Threshold and Intervals on the Probability of Failure of a Fail-Safe Structure

Figure 4: Failure of an Electronic Chip and a P-Version Finite-Element Analysis of the Failure Zone

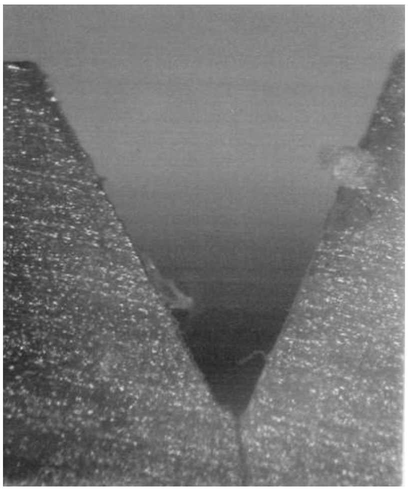

Figure 5: a V-notch Failure Analyzed by this Technique

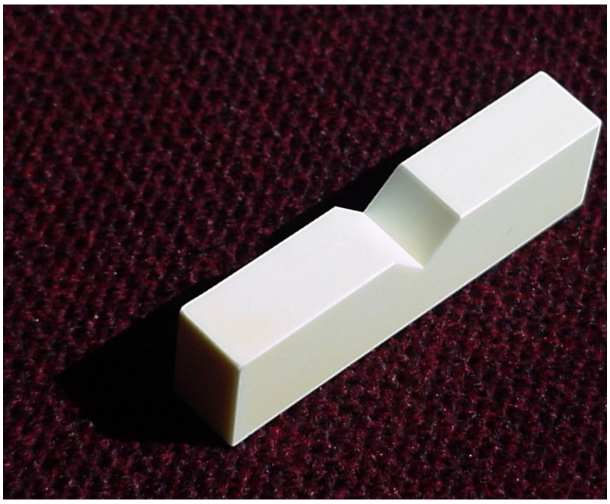

Figure 6: Alumina Notched Test Specimen

Figure 7: Galaxy Full-Scale Fatigue Test Aircraft

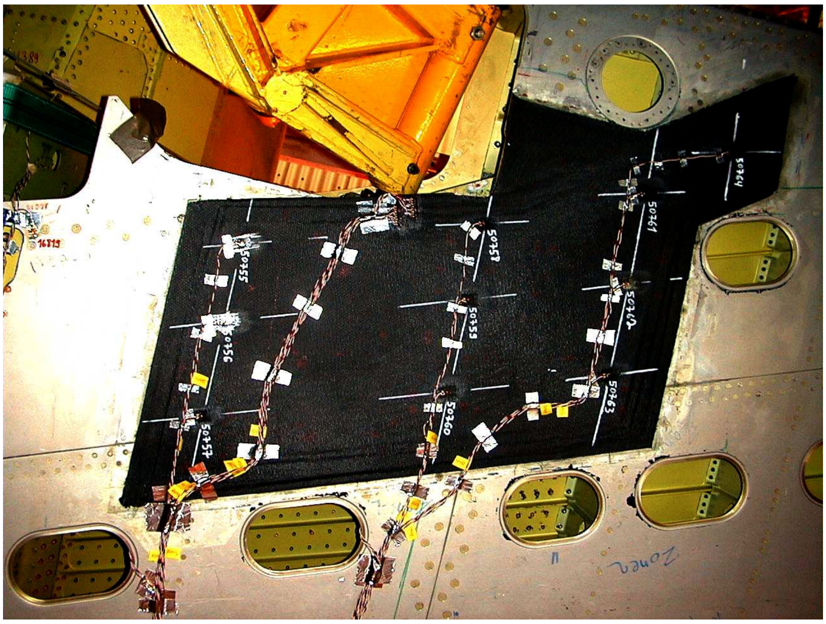

Figure 8: Composite Patch Applied to Lower Skin of RHS Fatigue Test Wing

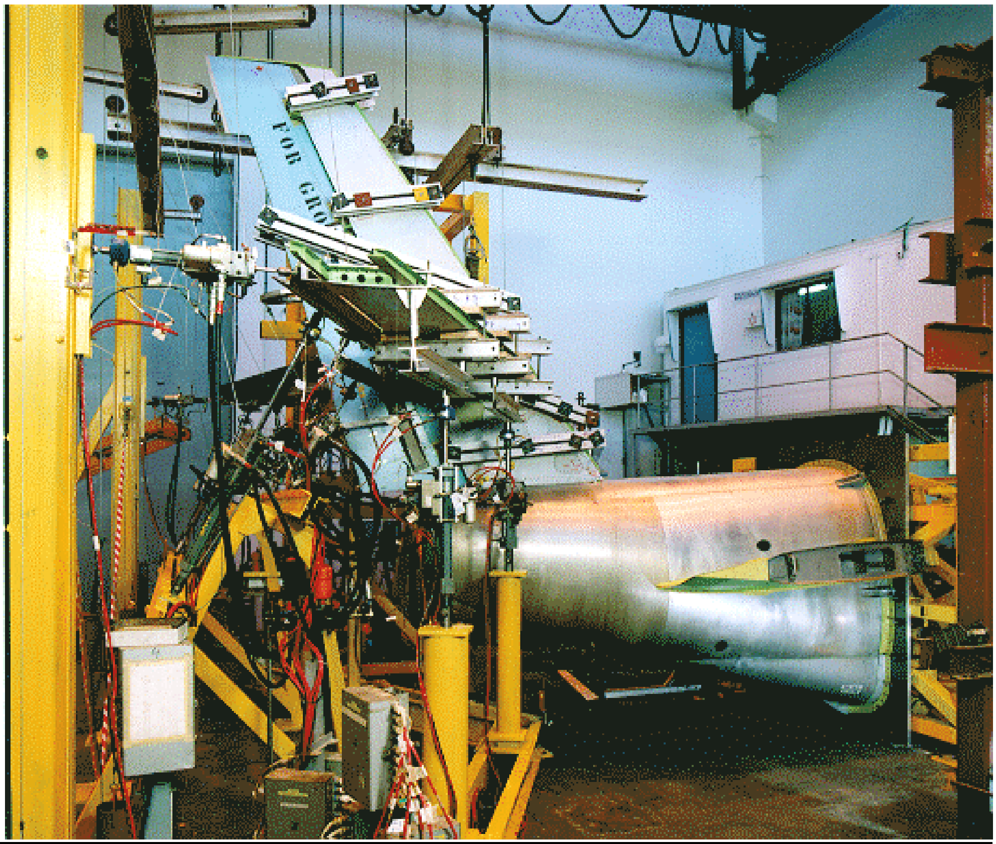

Figure 9: Galaxy Empennage – Fatigue and Damage-Tolerance Test

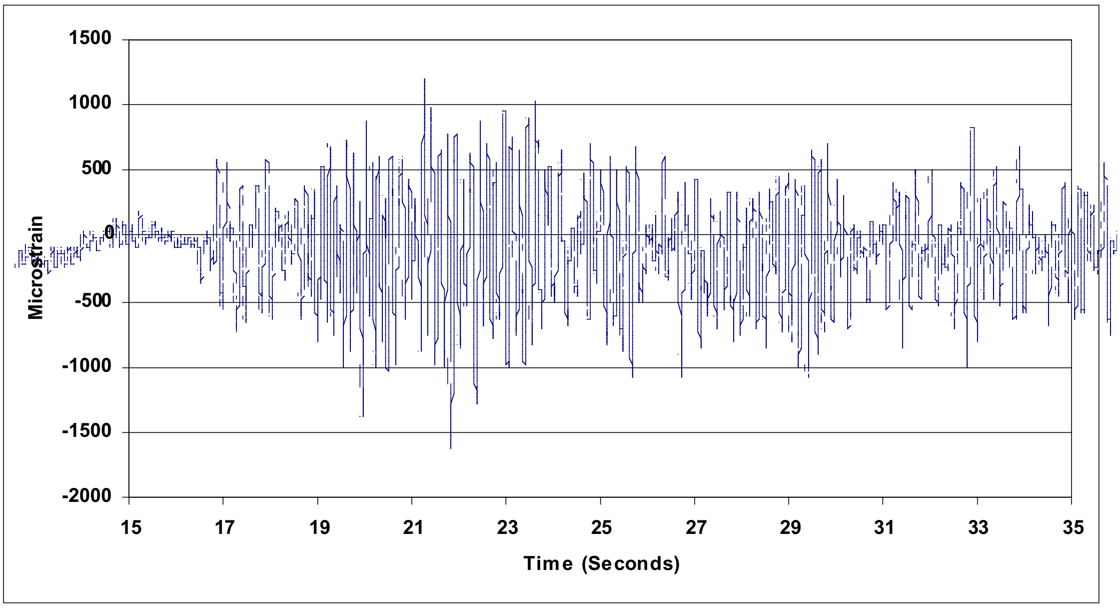

Figure 10: Measured Buffeting Loads on Horizontal Tail during Maximum Reverse Thrust

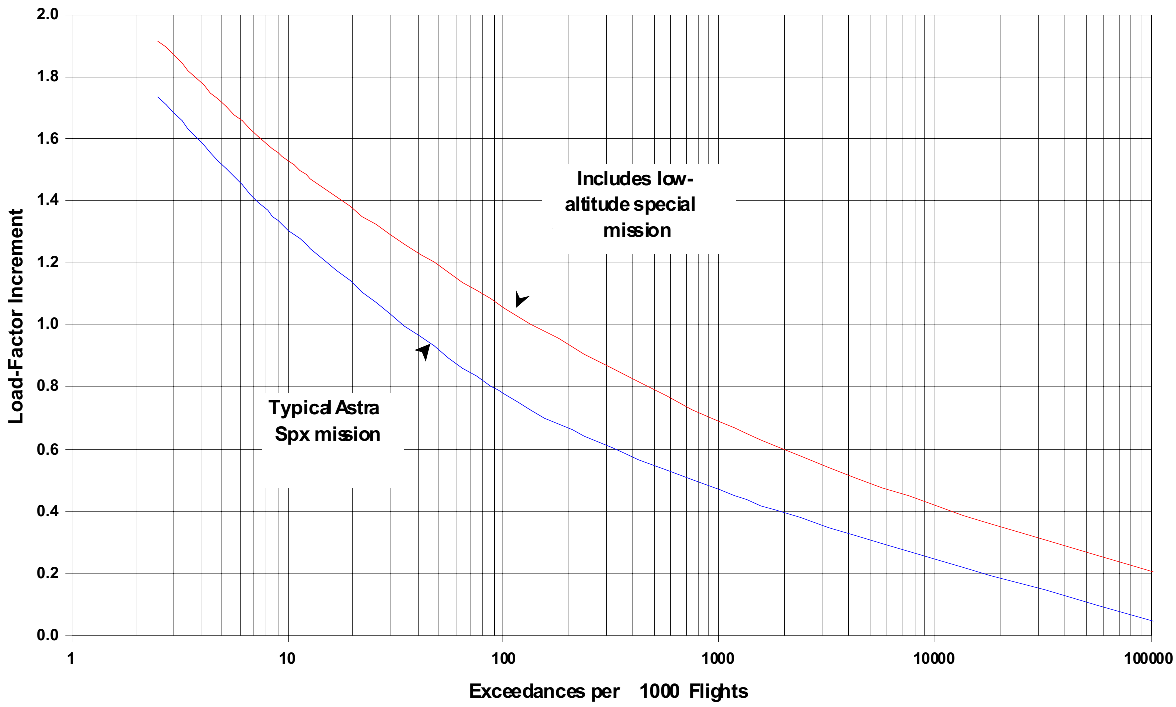

Figure 11: Gust Spectrum for Low-Altitude Astra Operation Compared to the Astra SPX Gust Spectrum

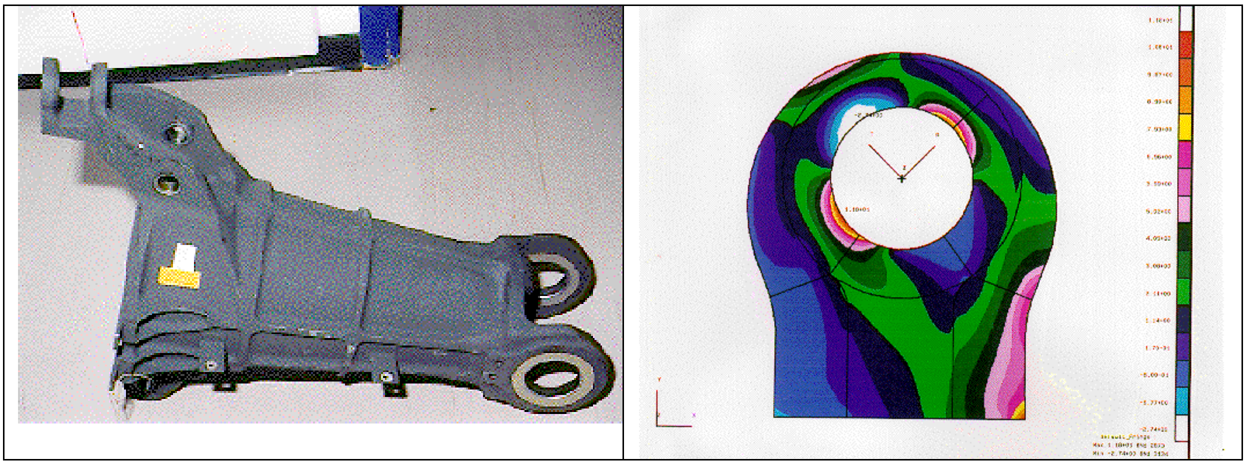

Figure 12: IAF AH-64A Apache Helicopter Pitch-Housing Component and Stress Distribution in Lug

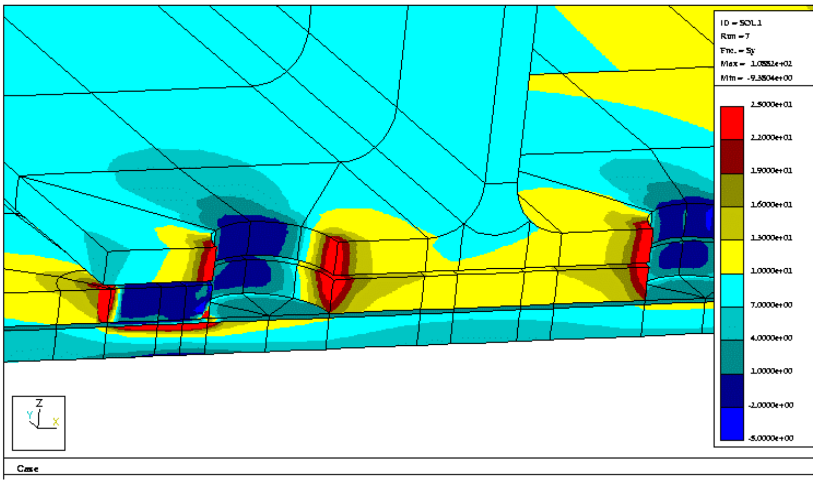

Figure 13: P-Version Finite-Element Model of a Skin to Frame Attachment Including a Crack by a Fastener Hole

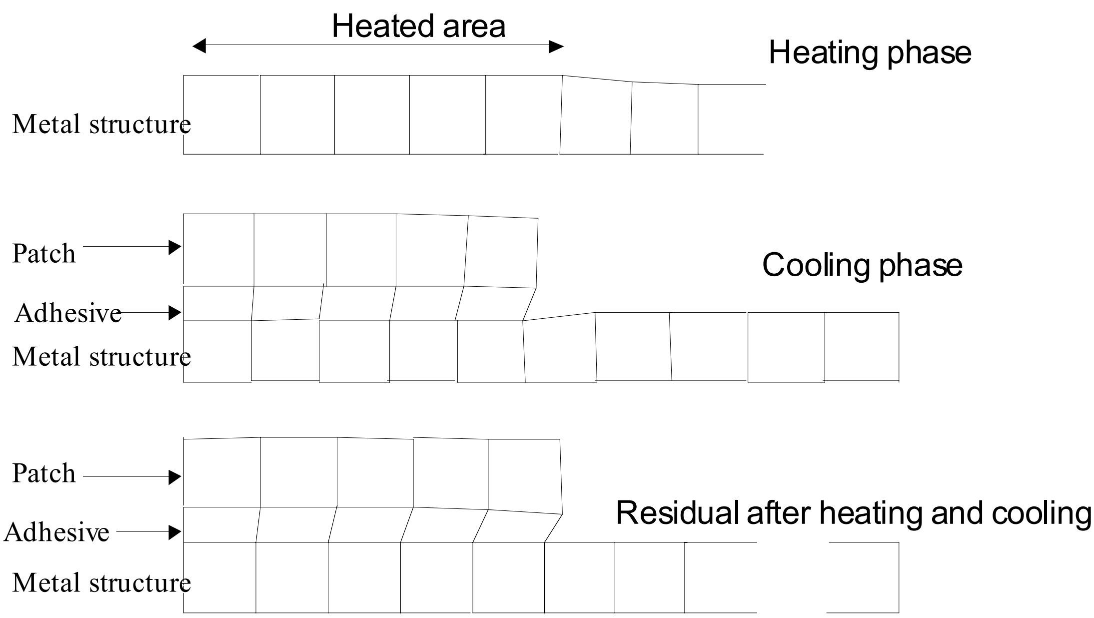

Figure 14: Schematic Representation of Residual Stresses Induced by Thermal Mismatch during the Application of a Composite Patch

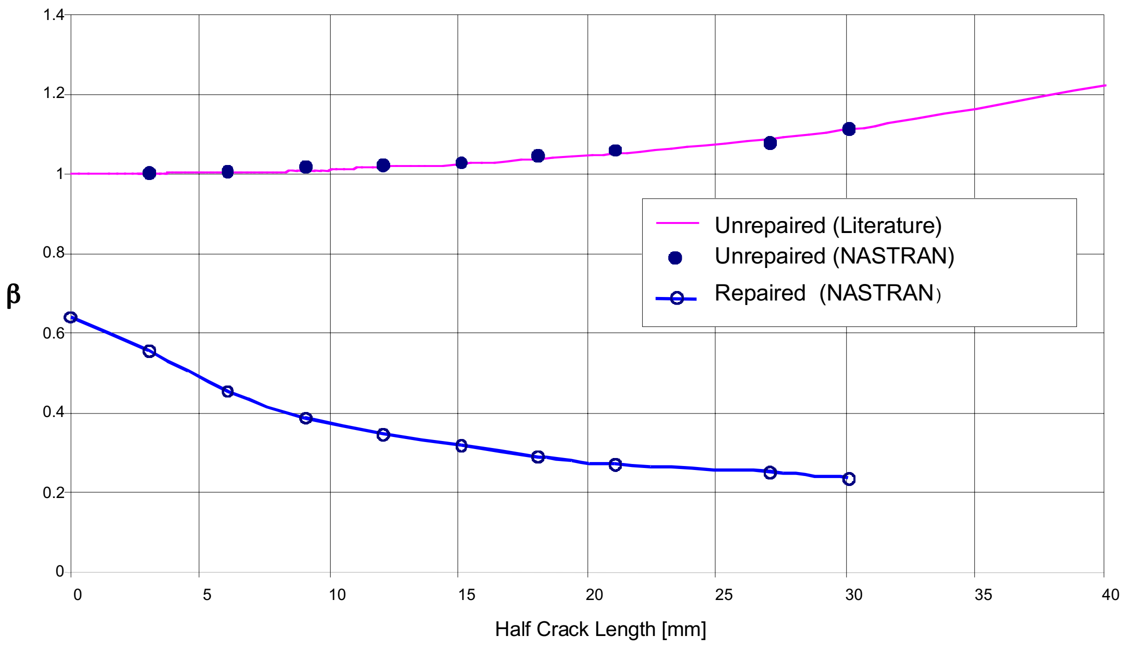

Figure 15: - Stress-Intensity Correction Factor for a Metallic Plate Repaired by a Composite Patch

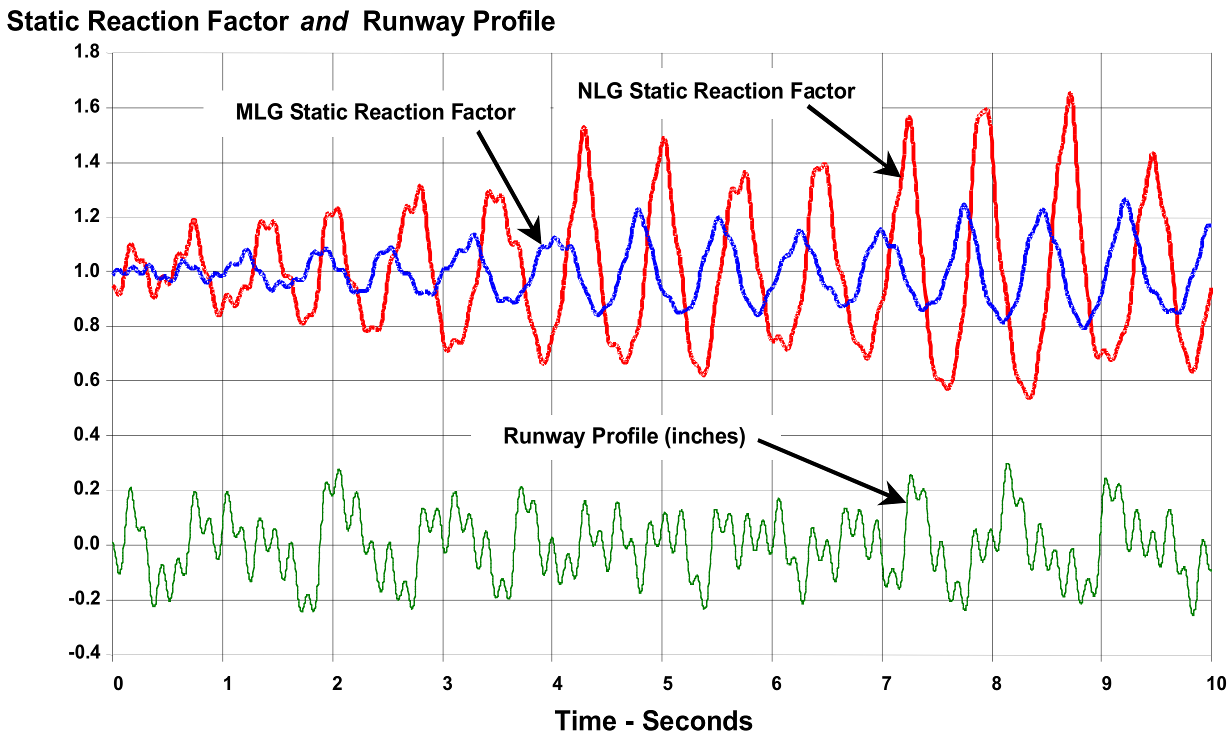

Figure 16: Landing Gear Normalized Reactions while Taxiing at 40 Knots

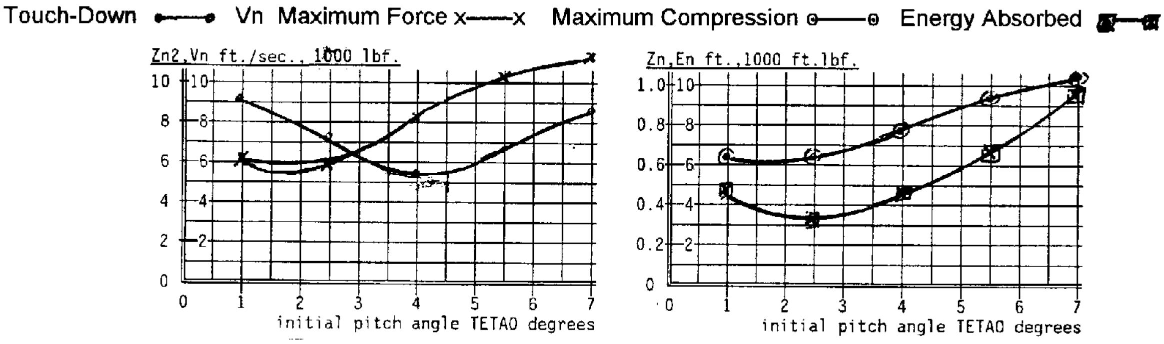

Figure 17: Nose Landing Gear Parameter Variation with Initial Tail-Down Angle

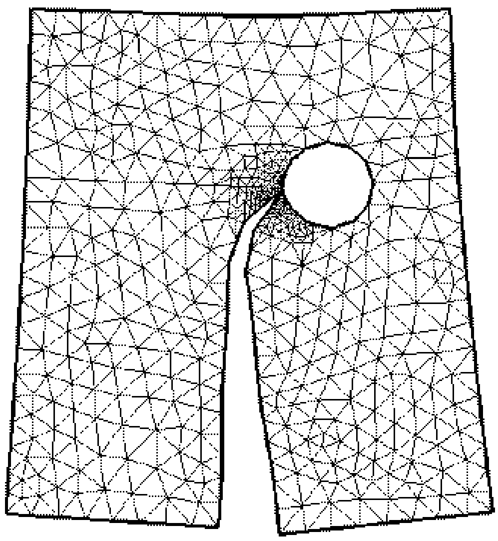

Figure 18: Finite-Element Analysis of a Crack Approaching a Hole
(Crack path and mesh in a deformed configuration)